Cell

Apoptotic Caspases Prevent the Induction of Type I Interferons by Mitochondrial DNA

Anthony Rongvaux,[1] Ruaidhrí Jackson,[1] Christian C.D. Harman,[1] Tuo Li,[2] A. Phillip West,[3] Marcel R. de Zoete,[1,7] Youtong Wu,[2] Brian Yordy,[1] Saquib A. Lakhani,[1,8] Chia-Yi Kuan,[5] Tadatsugu Taniguchi,[6] Gerald S. Shadel,[3,4] Zhijian J. Chen,[2,7] Akiko Iwasaki,[1,7] and Richard A. Flavell[1,7,*]

[1]Department of Immunobiology, Yale University School of Medicine, New Haven, CT 06520, USA
[2]Department of Molecular Biology, University of Texas Southwestern Medical Center, Dallas, TX 75390, USA
[3]Department of Pathology
[4]Departments of Genetics
Yale University School of Medicine, New Haven, CT 06520, USA
[5]Department of Pediatrics, Division of Neurology and The Center for Neurodegenerative Diseases (CND), Emory University School of Medicine, Atlanta, GA 30322, USA
[6]Department of Molecular Immunology, Institute of Industrial Science, The University of Tokyo, Tokyo 153-8505, Japan
[7]Howard Hughes Medical Institute
[8]Present address: Department of Pediatrics, University of South Dakota Sanford School of Medicine, Sioux Falls, SD 57117, USA
*Correspondence: richard.flavell@yale.edu
http://dx.doi.org/10.1016/j.cell.2014.11.037

SUMMARY

The mechanism by which cells undergo death determines whether dying cells trigger inflammatory responses or remain immunologically silent. Mitochondria play a central role in the induction of cell death, as well as in immune signaling pathways. Here, we identify a mechanism by which mitochondria and downstream proapoptotic caspases regulate the activation of antiviral immunity. In the absence of active caspases, mitochondrial outer membrane permeabilization by Bax and Bak results in the expression of type I interferons (IFNs). This induction is mediated by mitochondrial DNA-dependent activation of the cGAS/STING pathway and results in the establishment of a potent state of viral resistance. Our results show that mitochondria have the capacity to simultaneously expose a cell-intrinsic inducer of the IFN response and to inactivate this response in a caspase-dependent manner. This mechanism provides a dual control, which determines whether mitochondria initiate an immunologically silent or a proinflammatory type of cell death.

INTRODUCTION

Multicellular organisms are constantly exposed to the threat of viral infections. As a response, vertebrates have evolved several mechanisms of antiviral defense. These mechanisms include the production of type I interferons (IFNs) (Stetson and Medzhitov, 2006) and the suicide of infected cells (Upton and Chan, 2014).

Type I IFNs (IFNα and IFNβ) are cytokines of major importance for the innate antiviral response (Stetson and Medzhitov, 2006). They are produced after recognition of viral nucleic acids by toll-like receptors (TLRs) or by cytoplasmic proteins such as RIG-I-like receptors (RLRs) or the cyclic GMP-AMP synthase (cGAS) (Cai et al., 2014; Kawai and Akira, 2011; Loo and Gale, 2011). After their secretion, type I IFNs bind to the type I IFN receptor (IFNAR) in an autocrine and paracrine manner. This signal induces the expression of hundreds of interferon-stimulated genes (ISGs) in the responding cell (Schneider et al., 2014). Overall, ISGs have the capacity to interfere with every step of viral replication, and, as a consequence, the IFN response results in the establishment of a cellular state of viral resistance.

The programmed death of infected cells limits the possibility for viruses to subvert the cellular machinery for their own replication (Best, 2008; Yatim and Albert, 2011). One of the best-described mechanisms of programmed cell death is apoptosis, which is mediated through the activation of members of the caspase family of proteases (Fuchs and Steller, 2011; Kumar, 2007; Taylor et al., 2008). The mitochondrial pathway of apoptosis is induced in response to cellular stress. It is regulated by the activities of pro- and antiapoptotic members of the Bcl-2 family, which control the formation of the Bax/Bak channel that results in mitochondrial outer membrane permeabilization (MOMP) (Chipuk et al., 2010; Tait and Green, 2010; Youle and Strasser, 2008). Following MOMP, mitochondrial proteins, including cytochrome *c*, are released in the cytosol. Together with Apaf-1 and caspase-9, cytosolic cytochrome *c* forms a protein complex called the apoptosome, which induces the activation of caspase-9 (Jiang and Wang, 2004; Riedl and Salvesen, 2007). The downstream effector caspases-3 and -7 are cleaved and activated by caspase-9, triggering a cascade of proteolytic events that culminates in the demise of the cell through apoptosis (Kroemer et al., 2009).

Although caspases are key mediators of apoptotic cell death (Kumar, 2007), multiple mechanisms of caspase-independent cell death exist (Chipuk and Green, 2005; Tait et al., 2014; Vanden Berghe et al., 2014). The discovery of a broad diversity of

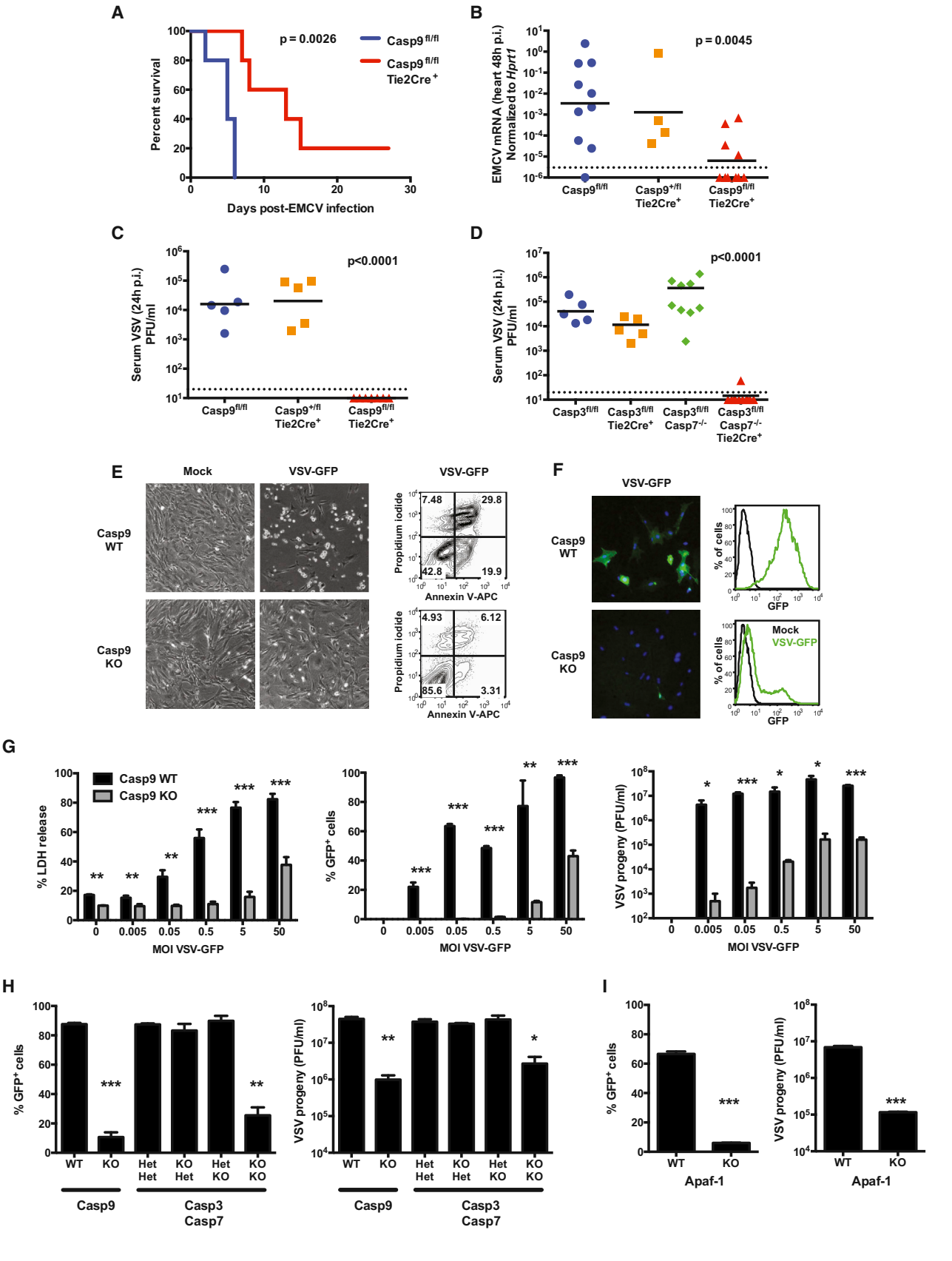

(legend on next page)

nonapoptotic death pathways has led to a re-evaluation of caspases as essential mediators of cell death. An appealing hypothesis to reconcile the evolutionary conservation of proapoptotic caspase signaling with the existence of multiple, and potentially redundant, death-inducing pathways is that caspase-dependent apoptosis is unique in its capacity to induce an immunologically silent form of cell death, whereas other types of cell death have proinflammatory or immunostimulatory properties (Martin et al., 2012; Tait et al., 2014). Indeed, necrotic cell death results in the release of molecules with proinflammatory properties, collectively termed damage-associated molecular patterns (DAMPs) or alarmins (Kroemer et al., 2013). Mounting evidence demonstrates that several DAMPs can be inactivated in a caspase-dependent manner during apoptosis, supporting the importance of caspases in maintaining cell death as immunologically silent. However, it is probable that a large spectrum of caspase-dependent mechanisms of immune regulation remain to be discovered (Martin et al., 2012).

In this study, we identify an unsuspected mechanism by which the mitochondrial events of apoptosis actively trigger the initiation of a cell-intrinsic immune response, mediated by the expression of type I IFNs. Proapoptotic caspases, activated simultaneously by mitochondria, are required to inhibit that response and to maintain apoptosis immunologically silent. Therefore, mitochondria and caspases play a crucial role not only in the decision of the cell to live or to commit suicide but also on the decision to die in an inflammatory or immunologically silent manner.

RESULTS

Intrinsic Apoptosis Deficiency Confers Resistance to Viral Infection

As mice with genetic deficiencies in the intrinsic pathway of apoptosis die perinatally (Hakem et al., 1998; Kuida et al., 1998; Lakhani et al., 2006; Yoshida et al., 1998), we generated mice with a floxed caspase-9 allele or a floxed caspase-3 allele (Figure S1A available online). With the initial objective of studying the role of the intrinsic pathway of apoptosis in immune cells, we crossed *Casp9*$^{fl/fl}$ mice and *Casp3*$^{fl/fl}$ *Casp7*$^{-/-}$ mice with Tie2-Cre(E+H) (Koni et al., 2001; Lakhani et al., 2006) to obtain mice with endothelial/hematopoietic tissue-specific deletion of the respective floxed alleles (Figures S1B–S1F). We observed that *Casp9*$^{fl/fl}$ Tie2-Cre^{+} and *Casp3*$^{fl/fl}$ *Casp7*$^{-/-}$ Tie2-Cre^{+} mice were highly resistant to viral infection in comparison to littermate controls. Indeed, lethality following intraperitoneal infection with encephalomyocarditis virus (EMCV, 2×10^3 $TCID_{50}$), which was observed in control mice 6 days after infection, was delayed in *Casp9*$^{fl/fl}$ Tie2-Cre^{+} mice (Figure 1A). The prolonged survival and resistance to EMCV infection was associated with lower viral loads in the heart 2 days after infection, with undetectable expression of the EMCV genome in half of the *Casp9*$^{fl/fl}$ Tie2-Cre^{+} mice (Figure 1B). Furthermore, the deletion of caspase-9 or of both caspases-3 and -7 resulted in undetectable viral titers of vesicular stomatitis virus (VSV, 10^6 PFU) after intranasal infection (Figures 1C and 1D), highlighting a potent antiviral state in vivo in proapoptotic caspase-deficient animals.

To determine whether this phenotype could be recapitulated in vitro, primary mouse embryonic fibroblasts (MEFs) isolated from caspase-9 knockout (KO) (Kuida et al., 1998) from caspase-3/-7 double-KO (Lakhani et al., 2006) and from Apaf-1 KO mice (Yoshida et al., 1998) were infected with VSV. We observed that caspase-9-deficient cells (Casp9 KO) were only modestly affected by the infection with a recombinant strain of VSV expressing the green fluorescent protein (VSV-GFP), whereas wild-type (WT) cells derived from littermate embryos (Casp9 WT) showed the typical phenotype of infected cells (cell rounding, detachment, and death; Figure 1E). Fluorescence microscopy and flow cytometry analysis showed that only a small fraction of Casp9 KO cells expressed virus-encoded GFP (Figure 1F). To further substantiate this observation, Casp9 WT and KO MEFs were infected with VSV-GFP at various multiplicities of infection (MOI). By measuring cell death (percentage of LDH released) and viral infection and replication (GFP expression and plaque-forming units), we observed that caspase-9 deficiency significantly reduced the susceptibility of cells to VSV infection at all MOIs tested (Figure 1G). Casp9 KO MEFs also displayed increased resistance to infection by EMCV (Figure S2A) or by herpes simplex virus type 2 (HSV-2) (Figure S2B). Similarly, Casp3/7 double-KO and Apaf-1 KO MEFs showed resistance to VSV infection comparable to that observed in Casp9 KO (Figures 1H and 1I). These results demonstrate that deficiency in the intrinsic pathway of apoptosis, downstream of

Figure 1. Loss of the Intrinsic Pathway of Apoptosis Enhances Resistance to Viral Infection

(A and B) *Casp9*$^{fl/fl}$ Tie2-Cre^{+} and control mice were infected intraperitoneally with EMCV (2×10^3 $TCID_{50}$), and the survival was monitored (n = 5 mice/group, p value calculated by Mantel-Cox test) (A); or the mice were sacrificed 48 hr postinfection (p.i.), and viral loads in the heart were measured by real-time RT-PCR (n = 4–10 mice/group, combined from three independent experiments, p value calculated by one-way ANOVA) (B). Each symbol represents an individual mouse, and the black horizontal bars indicate geometric means. The dashed line indicates the limit of detection of the assay.

(C and D) *Casp9*$^{fl/fl}$ Tie2-Cre^{+} (C), *Casp3*$^{fl/fl}$ *Casp7*$^{-/-}$ Tie2-Cre^{+} (D), and control mice were infected intranasally with VSV (10^6 PFU) and sacrificed 24 hr later. Viral loads were measured in the plasma by plaque-forming assay (n = 5–7 mice/group, combined from at least two independent experiments, p value calculated by one-way ANOVA).

(E and F) Casp9 WT and KO primary MEFs were infected in vitro with VSV-GFP (MOI = 0.5) and analyzed 24 hr later (E). The expression of virus-encoded GFP was analyzed by fluorescence microscopy (green, GFP; blue, counter-staining of nuclei with DAPI) or by flow cytometry (F).

(G) Casp9 WT and KO primary MEFs were infected with the indicated MOI of VSV-GFP and were assessed 24 hr later for cell death with LDH release assay (left), expression of GFP (middle), and viral progeny production by plaque assay (right). Results are presented as mean ± SD of triplicates, representative of at least three independent experiments.

(H and I) Casp3/7 double-KO (H) or Apaf-1 KO (I) and respective control primary MEFs were infected with VSV-GFP (MOI = 0.5), and GFP expression and viral progeny were measured as in (G) (mean ± SD of duplicates, representative of two experiments).

*p < 0.05, **p < 0.01, and ***p < 0.001 (two-tailed unpaired Student's t test, compared to respective WT or HetHet control).

See also Figures S1 and S2.

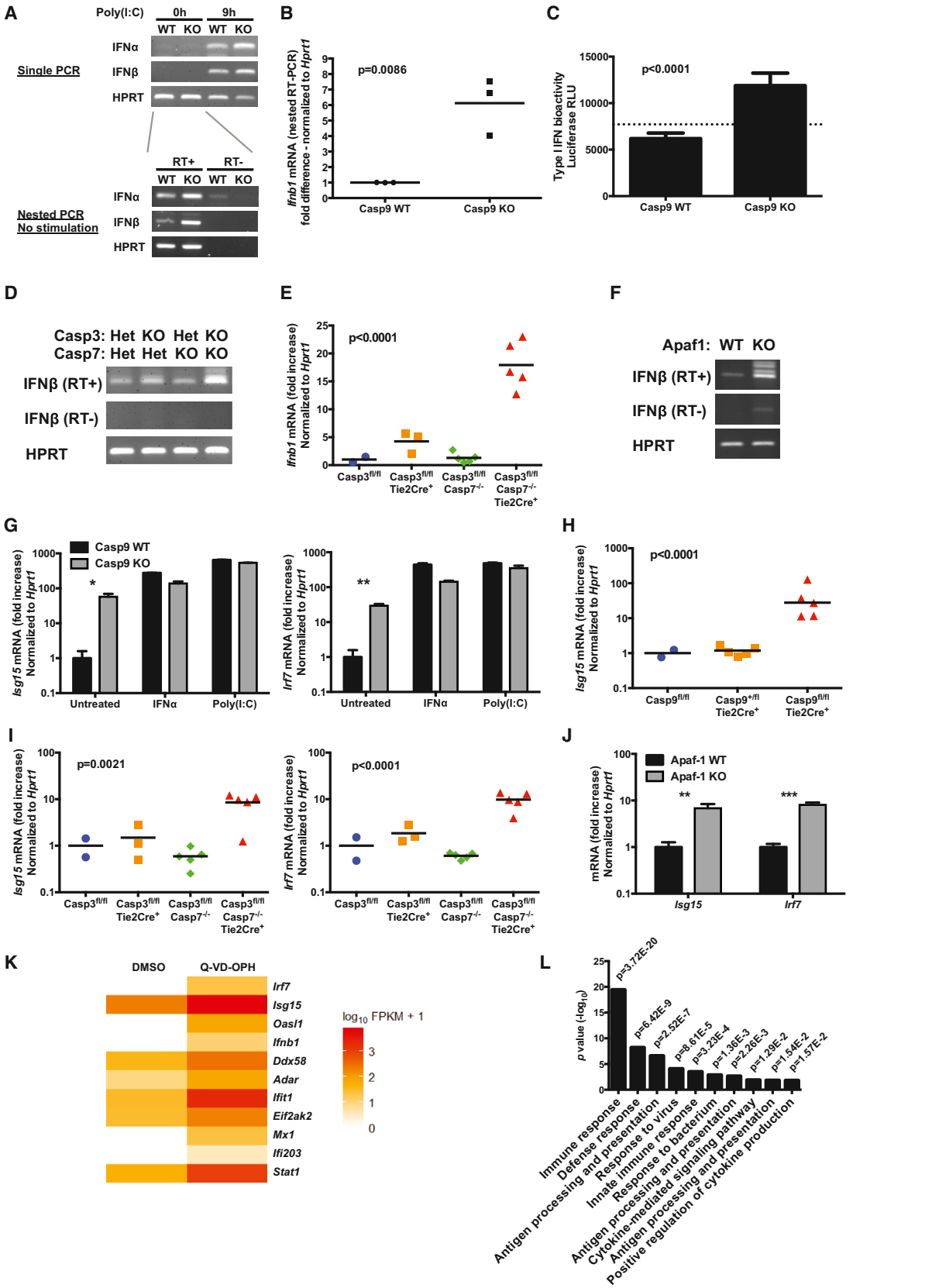

(legend on next page)

mitochondria, confers a strong broad-spectrum resistance to infection by RNA and DNA viruses, both in vivo and in vitro.

Constitutive Activation of the Type I IFN Response

Type I IFNs are critical determinants of the cellular susceptibility to viral infections. They are constitutively expressed at low levels, and these steady-state IFNs have profound physiological effects on homeostasis through tonic signaling in the absence of acute infection (Gough et al., 2012; Taniguchi and Takaoka, 2001). We measured the baseline expression levels of type I IFNs using a highly sensitive nested RT-PCR. We observed a modest increase in the basal levels of the mRNA encoding both IFNα and IFNβ in Casp9 KO MEFs compared to WT controls (Figure 2A) in the absence of any stimulation. We confirmed this result using a quantitative nested real-time PCR (Figure 2B), as well as a type I IFN bioactivity assay (Figure 2C). Increased steady-state type I IFN mRNA was also induced in vitro and in vivo by Casp3/7 double deficiency (Figures 2D and 2E), as well as by the absence of Apaf-1 in MEFs (Figure 2F).

In addition, we observed that interferon-stimulated genes (ISGs) were constitutively expressed at elevated levels in vitro and in vivo in Casp9 KO (Figures 2G, 2H, S3A, and S3B), in Casp3/7 double-KO (Figure 2I) and in Apaf-1 KO cells (Figure 2J) in the absence of any stimulation. The maximal expression level of these ISGs, as induced by IFNα or intracellular poly(I:C), was comparable between Casp9 WT and KO cells.

To determine whether the pharmacological inhibition of caspases could recapitulate the phenotype caused by genetic deficiencies, we treated WT MEFs with broad-spectrum inhibitors of caspases (Z-VAD-fmk, Boc-D-fmk, and Q-VD-OPH). These inhibitors induced an increased expression of ISGs (Figures 2K, S3C, and S3D), similar to the effect of caspase or Apaf-1 deficiency. Surprisingly, a gene ontology analysis of the genes differentially expressed between WT cells treated with dimethyl sulfoxide (DMSO) or Q-VD-OPH revealed a highly significant overrepresentation of pathways related to immune responses (Figure 2L). Although this transcriptional analysis does not take into account the direct proteolytic effects of caspases, it nevertheless reveals a profound effect of caspase inhibition on immune function.

Next, we compared the transcriptional changes induced by caspase inhibition in WT and IFNAR1 KO cells, which lack a critical subunit of the receptor for IFNα/β (Müller et al., 1994). We observed that the absence of the IFNAR receptor abrogated the transcriptional response of the cells to caspase inhibition by Q-VD-OPH (Figures 3A and S3D and Table S1), demonstrating the role of type I IFNs in this response.

To demonstrate that ISG expression and viral resistance in Casp9 KO cells was also due to type I IFNs, supernatants from confluent unstimulated Casp9 WT and KO MEFs were transferred to cultures of WT MEFs for 24 hr. The conditioned supernatant from Casp9 KO cells induced an increase in the expression of ISGs by WT MEFs (Figure 3B) to levels similar to those measured in Casp9 KO cells (compare with Figure 2G). Next, we pretreated WT cells with conditioned supernatants collected from Casp9 WT and KO cells in the absence or presence of neutralizing anti-IFNα/β antibodies. The cells were then washed and infected with VSV-GFP. The supernatants from Casp9 KO cell cultures conferred resistance to VSV infection in WT cells, and this effect was completely abolished by the presence of anti-IFNα/β neutralizing antibodies in the conditioned media during the pretreatment of the cells (Figure 3C). Similarly, conditioned supernatants from Casp9 KO cells failed to confer resistance to viral infection when used to pretreat IFNAR1 KO MEFs (Figure S4). These results demonstrate that the ISG-inducing activity and the resistance to VSV infection are mediated by the elevated concentrations of type I IFNs in the supernatant of Casp9 KO cells.

To further confirm this result, we generated Casp9/IFNAR1 double-KO MEFs. Like Casp9 KO cells, Casp9/IFNAR1 double-KO cells expressed increased steady-state levels of IFNα/β (Figure 3D), and their supernatant contained ISG-inducing

Figure 2. Inhibition of Intrinsic Apoptosis Activates the IFN Response

(A) The expression of IFNα and IFNβ mRNA was determined by RT-PCR in Casp9 WT and KO primary MEFs. Top: single RT-PCR on untreated cells and on cells transfected with poly(I:C) as a positive control. Bottom: nested RT-PCR on untreated cells (RT+, RNA reverse transcribed in cDNA; RT−, no reverse transcription).

(B) The steady-state expression of IFNβ mRNA expression in unstimulated primary MEFs was quantified by nested real-time RT-PCR. Each dot represents an independent experiment; p value: two-tailed unpaired Student's t test.

(C) Type I IFN bioactivity in the culture supernatant of unstimulated MEFs was measured using an ISRE-Luc reporter cell line (mean ± SD of six replicates, representative of two independent experiments; p value: two-tailed unpaired Student's t test; the dashed line indicates background from untreated reporter cells).

(D) Nested RT-PCR amplification of steady-state IFNβ in Casp3/7 double-deficient and control primary MEFs.

(E) IFNβ mRNA expression measured by real-time RT-PCR in Casp3/7-deficient and control spleen cells (n = 2–5 mice/genotype; p value calculated by one-way ANOVA).

(F) Nested RT-PCR amplification of steady-state IFNβ in Apaf-1 WT and KO primary MEFs.

(G) The expression of selected ISGs in Casp9 WT and KO primary MEFs was measured by real-time RT-PCR. IFNα and intracellular poly(I:C) were used as positive controls (mean ± SD of duplicates, representative of at least five independent experiments). *$p < 0.05$, **$p < 0.01$, and ***$p < 0.001$; two-tailed unpaired Student's t test.

(H and I) ISG mRNA expression was measured by real-time RT-PCR in Casp9-deficient and control white blood cells (H) or in Casp3/7 double-deficient and control spleen cells (I) (n = 2–5 mice/genotype; p value: one-way ANOVA).

(J) ISG mRNA expression measured by real-time RT-PCR in Apaf-1 WT and KO primary MEFs (mean ± SD of triplicates, representative of three independent experiments; p value calculated as in G).

(K) Heatmap of the expression of IFNβ and selected ISGs in WT primary MEFs stimulated for 48 hr with vehicle (DMSO) or with the caspase inhibitor Q-VD-OPH (10 μM).

(L) Gene Ontology analysis of the pathways overrepresented among genes differentially expressed between WT primary MEFs stimulated with vehicle or with Q-VD-OPH.

See also Figures S3 and S5 and Table S1.

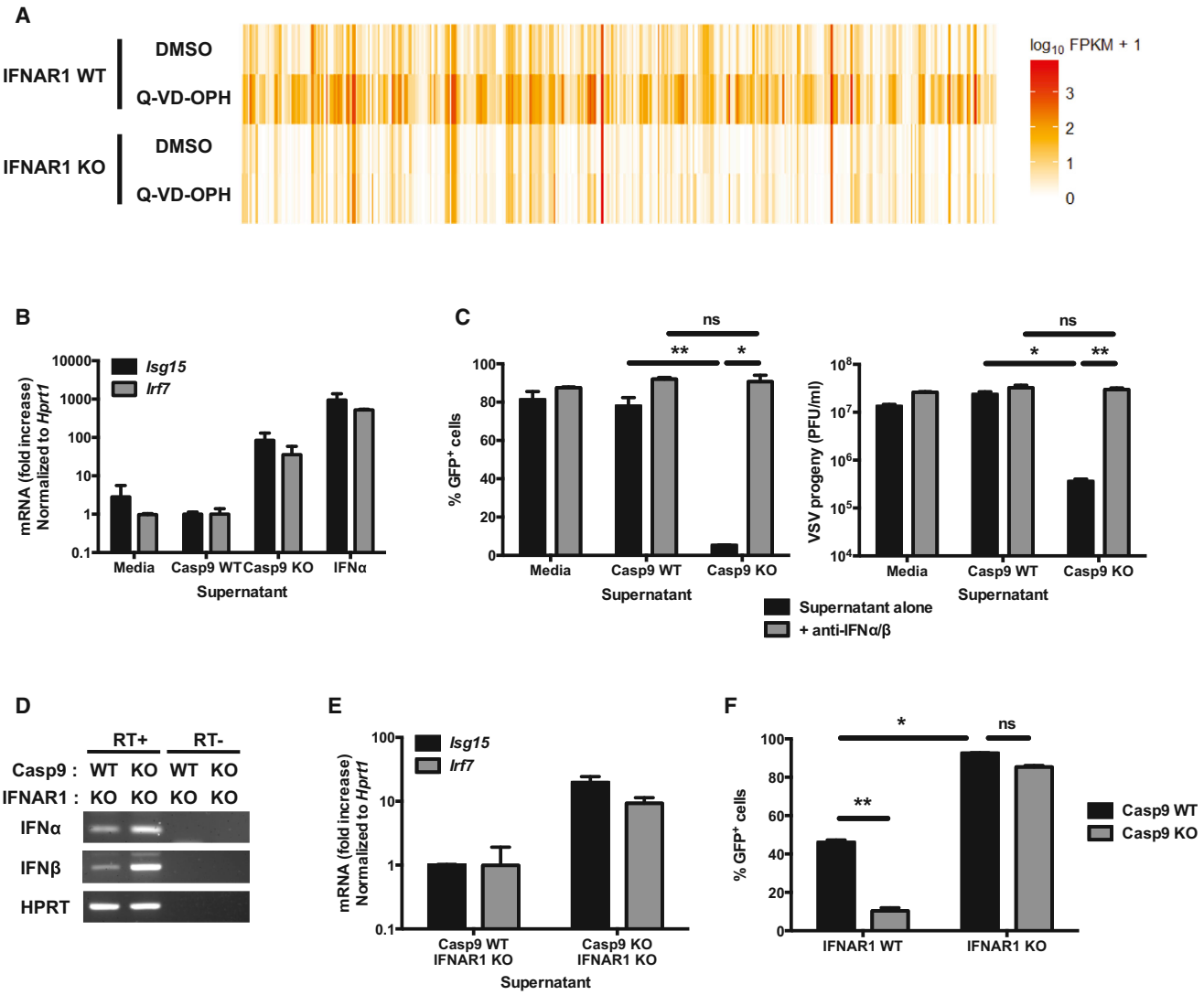

Figure 3. Expression of ISGs and Antiviral Resistance Is Mediated by Type I IFNs

(A) Heatmap of the expression of genes differentially expressed ($q < 0.05$, fold difference ≥ 5) in IFNAR1 WT and KO primary MEFs stimulated for 48 hr with vehicle (DMSO) or with the caspase inhibitor Q-VD-OPH (10 μM) and determined by RNA sequencing on duplicate samples.

(B) Culture supernatants of confluent cultures of Casp9 WT and KO primary MEFs were collected. WT primary MEFs were then incubated for 16 hr in the presence of these supernatants or of recombinant IFNα (50 U/ml), and the expression level of selected ISGs was measured by real-time RT-PCR (mean ± SD of duplicates; representative of two independent experiments).

(C) WT primary MEFs were incubated for 16 hr with conditioned supernatants from Casp9 WT or KO MEFs in the presence or absence of anti-IFNα and anti-IFNβ neutralizing antibodies (300 NU/ml each). The cells were then washed, infected with VSV-GFP (MOI = 0.5, 24 hr), and the expression of GFP (left) and viral progeny production (right) was measured (mean ± SD of triplicates, representative of three independent experiments).

(D) The expression of IFNα and IFNβ mRNA was detected by nested RT-PCR in unstimulated Casp9 WT/IFNAR1 KO and Casp9 KO/IFNAR1 KO primary MEFs (RT+, RNA reverse transcribed in cDNA; RT−, no reverse transcription).

(E) WT primary MEFs were incubated for 16 hr with conditioned media from Casp9/IFNAR1 WT/KO or KO/KO MEFs, and the expression levels of ISGs were measured by real-time RT-PCR.

(F) Casp9/IFNAR1 double-KO and control primary MEFs were infected with VSV-GFP (MOI = 0.5, 24 hr), and the expression of GFP was measured by flow cytometry (mean ± SD of duplicates, representative of three experiments).

*$p < 0.05$ and **$p < 0.01$; ns, not significant; pairwise comparisons following two-way ANOVA (C and F).

See also Figure S4 and Tables S1 and S2.

activity (Figure 3E). However, in the absence of IFNAR1, Casp9 WT and KO cells were equally susceptible to VSV infection (Figure 3F). As Casp9/IFNAR1 double-KO cells are deficient in apoptosis but are nevertheless susceptible to VSV, this result shows that viral resistance is not a direct consequence of defective cell death.

Caspase-9-deficient mice die during embryonic development or shortly after birth, and this phenotype has been attributed to apoptosis defects in the developing brain (Hakem et al., 1998; Kuida et al., 1998). However, we wanted to determine whether the constitutive activation of the IFN response and high expression of ISGs could contribute to this lethality. To this end, we compared the viability of caspase-9 KO mice in pre- and postnatal life in the presence or absence of IFNAR1 (Table S2). The absence of IFNAR1 did not rescue the embryonic lethality, showing that constitutive type I IFNs/ISGs expression is not responsible.

Aberrant expression of type I IFNs is the cause of several autoimmune disorders (Stetson, 2009). Surprisingly, however, despite constitutive expression of type I IFNs and ISGs, conditional Casp9 KO or Casp3/7 double-KO mice did not show any increase in total serum immunoglobulin or in antinuclear antibodies, two diagnostic characteristics of autoimmune diseases (Figure S5). We speculate that this absence of autoimmunity despite constitutive IFN response is due to pleiotropic functions of caspases and probable functional deficiencies in other mechanisms involved in the development of (auto)immunity.

Taken together, these observations demonstrate that, in the absence of a functional pathway of intrinsic apoptosis, an increased expression of steady-state type I IFNs is sufficient to induce ISG expression, and viral resistance is established. Such unexpected findings raise the intriguing questions as to what ligands and mechanisms govern type I IFN response in dying cells, how healthy cells contain unwanted IFN production, and finally, by what means proapoptotic caspases affect these processes.

Bax/Bak-Dependent Induction of Type I IFNs

The intrinsic pathway of apoptosis is activated upon MOMP by the Bax/Bak channel (Jiang and Wang, 2004). We thus wanted to determine whether mitochondria and Bax/Bak-dependent permeabilization were also involved in regulating the IFN response. Unlike deficiency in Apaf-1 or caspases, the absence of Bax and Bak (Figures 4A and 4B) or the overexpression of the antagonist protein Bcl-2 (Figure S6A), although preventing cell death induced by viral infection (Figures 4A, 4B, S6B, and S6C), did not confer any resistance to viral infection (Figures 4B and S6C). This observation could suggest that Apaf-1 and caspases regulate IFN expression independently of mitochondrial events. However, further investigations revealed a more subtle role of Bax and Bak in this process. Indeed, unlike WT cells, Bax/Bak-deficient cells treated with the caspase inhibitor Q-VD-OPH failed to induce the expression of ISGs (Figure 4C). This observation suggests that Bax/Bak are actually required for the induction of the IFN response in the absence of active caspases. As Bax/Bak-dependent permeabilization of mitochondrial outer membrane occurs in cultures of unstimulated cells in only a small percentage of dying cells or in cells undergoing incomplete MOMP, we hypothesized that the pharmacological inhibition of Bcl-2 could favor Bax/Bak-dependent MOMP and amplify the IFN response caused by caspase deficiency or inhibition. Consistently, we observed an induction of the expression of IFNβ in Casp9 KO cells treated with the Bcl-2 inhibitor ABT-737 (Oltersdorf et al., 2005) (Figure 4D). In contrast, Casp9 WT cells did not express IFNβ in response to Bcl-2 inhibition, showing the role of caspases in regulating this response. As the constitutive expression of ISGs in Casp9 KO (Figures 2 and S3) could contribute to the response, we next treated WT cells with a combination of the Bcl-2 inhibitor ABT-737 and the caspase inhibitor Q-VD-OPH. The combination of Bcl-2/caspase inhibition (ABT-737 + Q-VD-OPH) resulted in a robust expression of IFNβ after 3–6 hr of stimulation (Figure 4E). Other cytokines, such as IL-6 and TNFα, were only moderately induced (Figure S6D). The induction of IFNβ mRNA by Bcl-2/caspase coinhibition was entirely dependent on the presence of Bax/Bak (Figure 4F). The treatment of human PBMCs with ABT-737 and Q-VD-OPH also induced high expression of IFNβ (Figure 4G), showing that the mechanism of Bax/Bak-dependent caspase-regulated induction of type I IFN is conserved between species. Importantly, inhibiting caspases in the context of cell-extrinsic, caspase-8-dependent apoptosis induction did not induce the expression of IFNβ, showing the specificity of this process for mitochondria-dependent apoptosis (Figure S6E).

Taken together, these results uncover an immunomodulatory role for the mitochondria in innate immunity, a process tightly regulated by proapoptotic caspases in which Bax/Bak-induced MOMP facilitates the release of a mitochondrial factor with the capacity to stimulate type I IFN expression and promote viral resistance.

Activation of the cGAS/STING Pathway

To identify the putative mitochondrial factor that induces type I IFN expression in response to Bcl-2/caspases coinhibition, we first determined which interferon-inducing pathway is involved. We used two criteria to determine the involvement of a candidate sensor or signaling molecule in this process: (1) the activation of this candidate factor after ABT-737 + Q-VD-OPH treatment and (2) the absence of IFNβ expression, in response to the same treatment, in cells lacking the candidate factor.

Interferon regulatory factors (IRFs), and in particular IRF-3 and IRF-7, are major transcription factors required for the expression of type I IFNs (Tamura et al., 2008), and they are activated by the upstream kinase TBK1. Consistent with the expression of IFNβ, the inhibition of Bcl-2 and caspases (ABT-737 + Q-VD-OPH) induced the phosphorylation of TBK1 and IRF-3 in Bax/Bak-sufficient cells, but not in Bax/Bak KO cells (Figure 5A). The phosphorylation of TBK1 and IRF-3 after transfection of HT-DNA (herring testes DNA, a stimulator of the interferon response that serves as a positive control) was not affected by the absence of Bax/Bak. The expression of IFNβ in response to ABT-737 + Q-VD-OPH was completely abrogated in IRF-3/7 double-deficient cells (Figure 5B). These results demonstrate the critical involvement of TBK1 and IRFs in Bax/Bak-dependent caspase-regulated type I IFN induction. Two intracellular pathways converge on the TBK1/IRFs-dependent transcription of type I IFNs: the RLR/MAVS-dependent pathway activated by intracellular viral RNA (Loo and Gale, 2011) and the cGAS/STING pathway of cytosolic DNA recognition (Cai et al., 2014). MAVS deficiency did not affect the response to ABT-737 + Q-VD-OPH (Figure 5C), excluding a role of the cytosolic RNA recognition pathway. In contrast, the Bax/Bak-dependent, caspase-regulated IFN production was entirely dependent on the cGAS/STING pathway of cytosolic DNA recognition. The cGAS/STING

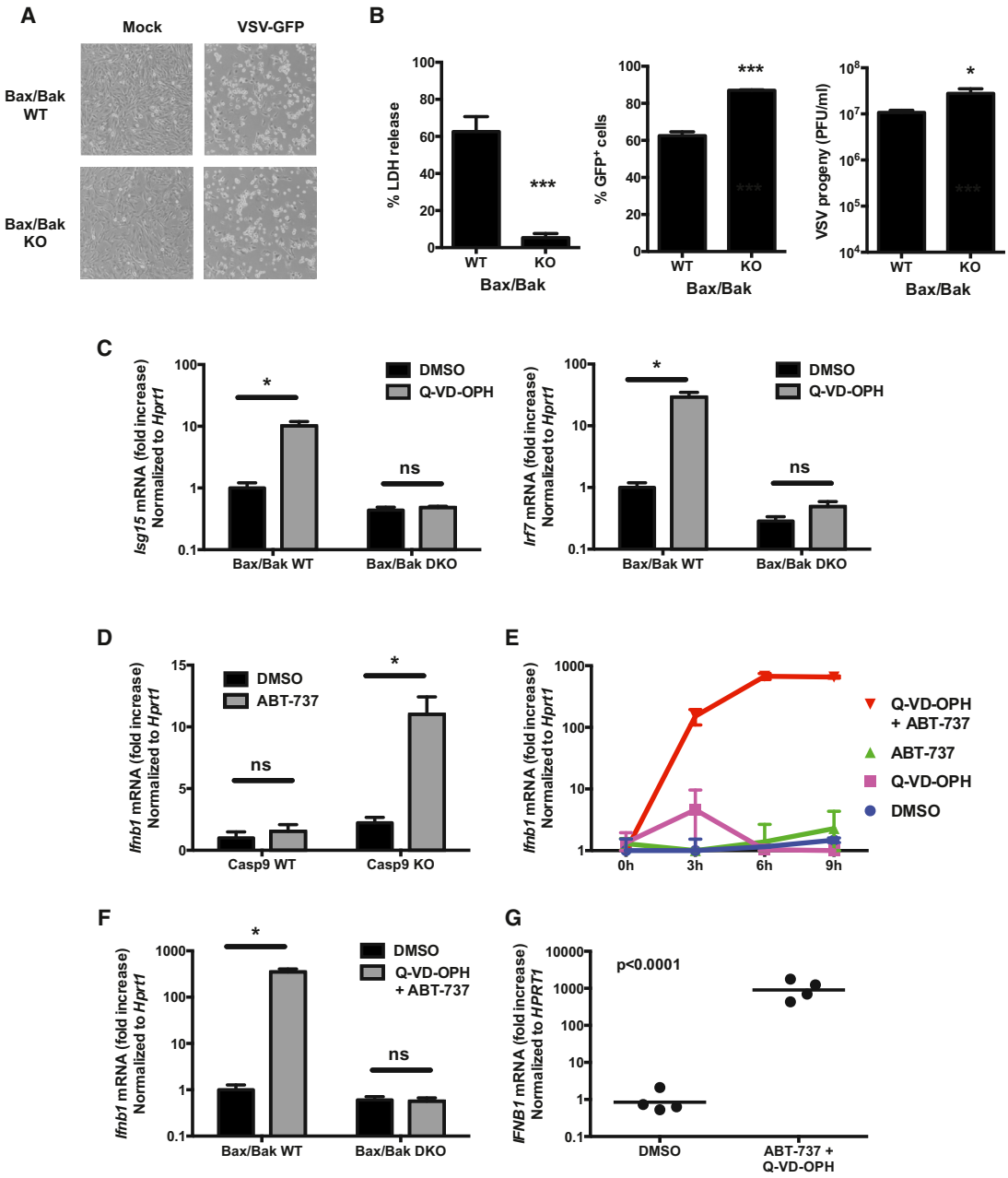

Figure 4. Bax/Bak-Dependent Induction of the IFN Response in the Absence of Active Caspases

(A and B) Bax/Bak double-KO and control immortalized MEFs were infected with VSV-GFP (MOI = 0.5). Their morphology was observed by microscopy (A); cell death, GFP expression, and viral progeny production were determined (B) (mean ± SD of triplicates, representative of three experiments).

*$p < 0.05$ and ***$p < 0.001$ (two-tailed unpaired t test).

(C) Bax/Bak WT and double-KO MEFs were treated with vehicle (DMSO) or with the caspase inhibitor Q-VD-OPH (10 μM), and the expression of ISGs was measured 48 hr later by RT-PCR (mean ± SD of triplicates, representative of three experiments).

(D) Expression of IFNβ mRNA by Casp9 WT and KO immortalized MEFs after 6 hr of treatment with vehicle (DMSO) or with the Bcl-2 inhibitor ABT-737 (10 μM) (mean ± SD of triplicates, representative of three independent experiments).

(E) Expression of IFNβ mRNA by WT primary MEFs at the indicated time points after stimulation with vehicle (DMSO), Bcl-2 inhibitor (ABT-737, 10 μM), caspase inhibitor (Q-VD-OPH, 10 μM) or both inhibitors (mean ± SD of duplicates, representative of three independent experiments).

(F) Expression of IFNβ mRNA by Bax/Bak WT and double-KO immortalized MEFs after 6 hr of treatment with vehicle or ABT-737 + Q-VD-OPH (mean ± SD of triplicates, representative of three independent experiments).

(G) Expression of IFNβ mRNA by human PBMCs after 6 hr of treatment with vehicle or ABT-737 + Q-VD-OPH (n = 4 healthy donors, results combined from 2 independent experiments; p value calculated by two-tailed unpaired Student's t test).

*$p < 0.05$; ns, not significant; pairwise comparisons following two-way ANOVA (C, D, and F). See also Figure S6.

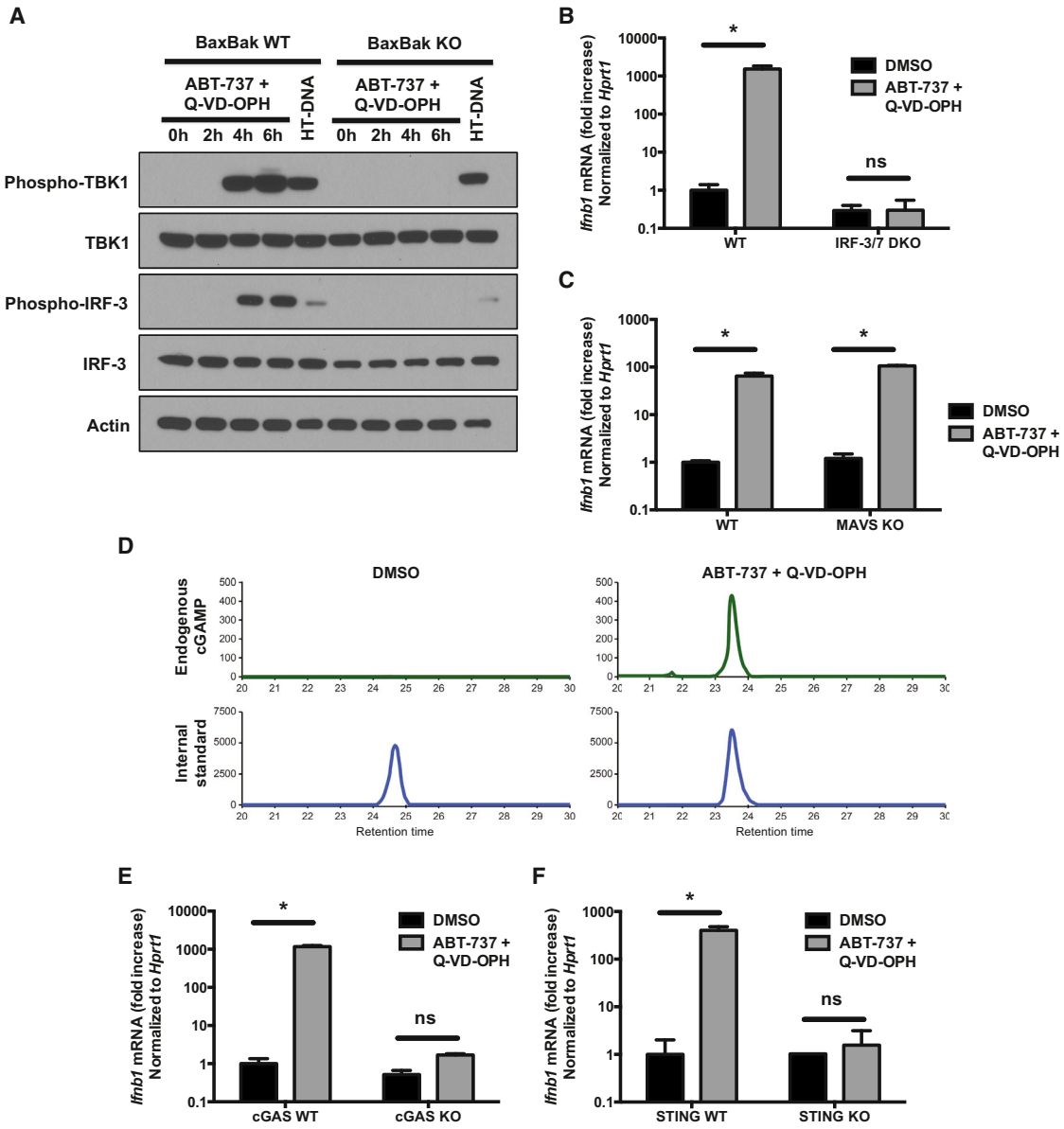

Figure 5. Activation of the cGAS/STING Pathway of IFN Induction

(A) Western blot analysis of the phosphorylation of TBK1 and IRF-3 in Bax/Bak WT and double-KO cells treated with combined Bcl-2/caspase inhibitors (ABT-737 + Q-VD-OPH, 10 μM each), or transfected with HT-DNA as a positive control (3 μg/ml, 3 hr). Result representative of three independent experiments.

(B and C) Expression of IFNβ mRNA by IRF-3/7 double-KO (B), MAVS KO (C), and control WT primary MEFs after 6 hr of treatment with vehicle (DMSO) or with ABT-737 + Q-VD-OPH (mean ± SD of triplicates, representative of two experiments).

(D) cGAMP measurement in cell extracts of WT primary MEFs stimulated for 4 hr with vehicle (DMSO) or ABT-737 + Q-VD-OPH. Result representative of two independent experiments.

(E and F) Expression of IFNβ mRNA by cGAS WT and KO bone-marrow-derived macrophages (E) and by STING WT and KO primary MEFs (F) after 6 hr of treatment with vehicle or ABT-737 + Q-VD-OPH (mean ± SD of three or two replicates, respectively).

*$p < 0.05$; ns, not significant; pairwise comparisons following two-way ANOVA (B, C, E, and F). See also Figure S7.

pathway is induced upon recognition of double-stranded DNA by cGAS (Cai et al., 2014). cGAS then acquires its enzymatic activity and synthesizes cGAMP, a dinucleotide that binds to and activates STING. The treatment with ABT-737+Q-VD-OPH resulted in detectable amounts of cGAMP in cell extracts, indicative of cGAS activity (Figure 5D). Furthermore, cGAS deficiency or STING deficiency completely prevented the IFNβ response to ABT-737 + Q-VD-OPH (Figures 5E and 5F). In contrast, TLR signaling was dispensable for the response to ABT-737 + Q-VD-OPH (Figure S7). These results unequivocally identify cGAS/STING as the pathway through which type I IFNs are induced by Bcl-2/caspase coinhibition.

Next, we determined whether the cGAS/STING/TBK1/IRFs pathway was also responsible for the increased steady-state IFN response in caspase-deficient cells. Interestingly, we observed constitutive phosphorylation of TBK1 in Casp9 KO cells, and this phosphorylation could be further induced by treatment with ABT-737 or transfected HT-DNA (Figure 6AFigure 6). That observation prompted us to test whether other components of the pathway are constitutively active in the absence of functional caspases. Upon stimulation, IRF-3 is ubiquitinylated and degraded through a process of negative feedback loop (Saitoh et al., 2006). We observed lower levels of total IRF-3 protein in Casp9 KO cells, which is suggestive of constitutive activation followed by degradation of IRF-3 (Figure 6A). Similarly, activated STING is phosphorylated and marked for lysosomal degradation (Konno et al., 2013). Again suggestive of constitutive activation, STING protein abundance was reduced in Casp9 KO cells, and the level of STING could be restored to WT levels after treatment with chloroquine, a potent inhibitor of lysosomal acidification (Figure 6B). These observations suggest that the STING pathway is constitutively active in Casp9 KO cells and likely contributes to the IFN-dependent induction of ISG expression. Furthermore, the constitutive activation of STING suggests that the inhibitory activity of caspases acts upstream of STING activation.

We next confirmed the role of the STING pathway at the genetic level. Similarly to the response to ABT-737+Q-VD-OPH, the constitutive expression of ISGs in Casp9 KO cells or in cells treated for 48 hr with the caspase inhibitor Q-VD-OPH was entirely abrogated in cells deficient for IRF-3/7, STING, or cGAS (Figures 6C–6E). In contrast, the RNA recognition pathway was not involved, as the expression of ISGs was not affected by MAVS deficiency (Figure 6F).

Taken together, these results demonstrate that the putative mitochondrial factor released after MOMP and that induces type I IFN in the absence of caspases is a ligand for the cytosolic DNA sensor cGAS. These observations demonstrate the existence of a regulated mechanism of activation of the cGAS pathway by an endogenous ligand. This ligand is sequestered in mitochondria in healthy cells, it is released in a Bax/Bak-dependent manner in dying cells, and its function is intrinsically regulated in a caspase-dependent manner.

mtDNA-Dependent Expression of Type I IFNs

We hypothesized that the mitochondrial ligand recognized by the DNA sensor cGAS could be mitochondrial DNA (mtDNA). To test this possibility, we used a well-established protocol of ethidium bromide (EtdBr)-mediated depletion of mtDNA (Hashiguchi and Zhang-Akiyama, 2009). The addition of low concentrations of EtdBr (150–450 ng/ml) to the culture medium results in the intercalation of EtdBr into mtDNA and prevents its replication, but it does not affect the replication of genomic DNA. This treatment induced an ~10-fold reduction in mtDNA (Figure 7A). When we treated mtDNA-depleted cells with both Bcl-2 and caspase inhibitors, the expression of IFNβ was strongly inhibited compared to control cells (Figures 7B and 7C). The phosphorylation of TBK1 and IRF-3 in response to the combined inhibitors was also abolished in mtDNA-depleted cells (Figure 7D). These results implicate mtDNA as the major inducer of type I IFN in this system. In contrast, the response to transfected HT-DNA was not affected by the EtdBr treatment (Figures 7B and 7C), showing that the cGAS/STING pathway remained functional. The response to other stimuli, such as transfected poly(I:C) and lipopolysaccharide (LPS), was also maintained after EtdBr treatment (Figure 7C), showing that other platforms of innate immune activation are unaffected by EtdBr treatment and mtDNA depletion. The expression of IFNβ by Casp9 KO cells in response to Bcl-2 inhibition and the constitutive phosphorylation of TBK1 in unstimulated Casp9 KO cells were also abrogated after depletion of mtDNA with EtdBr (Figures 7E and 7F).

Similarly to the response to ABT-737+Q-VD-OPH, the constitutive expression of ISGs in Casp9 KO cells was reversed by the treatment with EtdBr (Figure 7G), again implicating a role for mtDNA. We confirmed this result with an independent protocol of mtDNA depletion: dideoxycytidine (ddC) is an inhibitor of mitochondrial DNA polymerase γ and does not affect the function of nuclear DNA polymerases (Kaguni, 2004). ddC efficiently depleted mtDNA and reduced the expression of ISGs (Figure 7H), similar to the EtdBr treatment.

Together, these results show that mtDNA is an endogenous ligand that is released from mitochondria via Bax/Bak and that induces type I IFN expression through the cGAS/STING pathway. Caspases play a crucial role in preventing this cell-intrinsic immune response, thus maintaining the immunologically silent nature of mitochondria-dependent apoptotic cell death (Figure 7I).

DISCUSSION

The physiological role of regulated cell death is to maintain homeostasis, and dysregulated cell death can result in cancer, autoimmune and inflammatory disorders, immunodeficiency, or neurodegeneration. The highly regulated process of caspase-dependent apoptosis is unique in its capacity to induce a noninflammatory type of cell death (Martin et al., 2012; Tait et al., 2014). In contrast, caspase-independent cell death generally induces an inflammatory response through release of molecules, termed DAMPs, into the extracellular environment. These DAMPs contribute to the recruitment and activation of inflammatory cells of the immune system such as granulocytes and monocytes/macrophages. Here, we identify a mechanism by which dying cells expose an intracellular DAMP that activates a cell-intrinsic innate immune response. This type of cell-intrinsic immune activation in dying cells could occur while the physical integrity of the plasma membrane is still intact or even in cells that will eventually recover and will not undergo death.

Another singular aspect of this process is the dual role played by mitochondria. Mitochondrial membrane permeabilization is a point of no return in the decision to initiate cell suicide. Bax/Bak-dependent apoptosis is generally considered as a noninflammatory type of cell death. However, our results show that Bax and Bak contribute actively to the induction of the IFN response. The concomitant activation of caspases is required to maintain this type of cell death immunologically silent. This mechanism likely provides the cell with an additional level of control over the decision of whether to die with or without alerting the immune system. One physiological situation in which Bax/Bak-dependent induction of type I IFNs could occur is in the context of infection by viruses that express caspase inhibitors (Best,

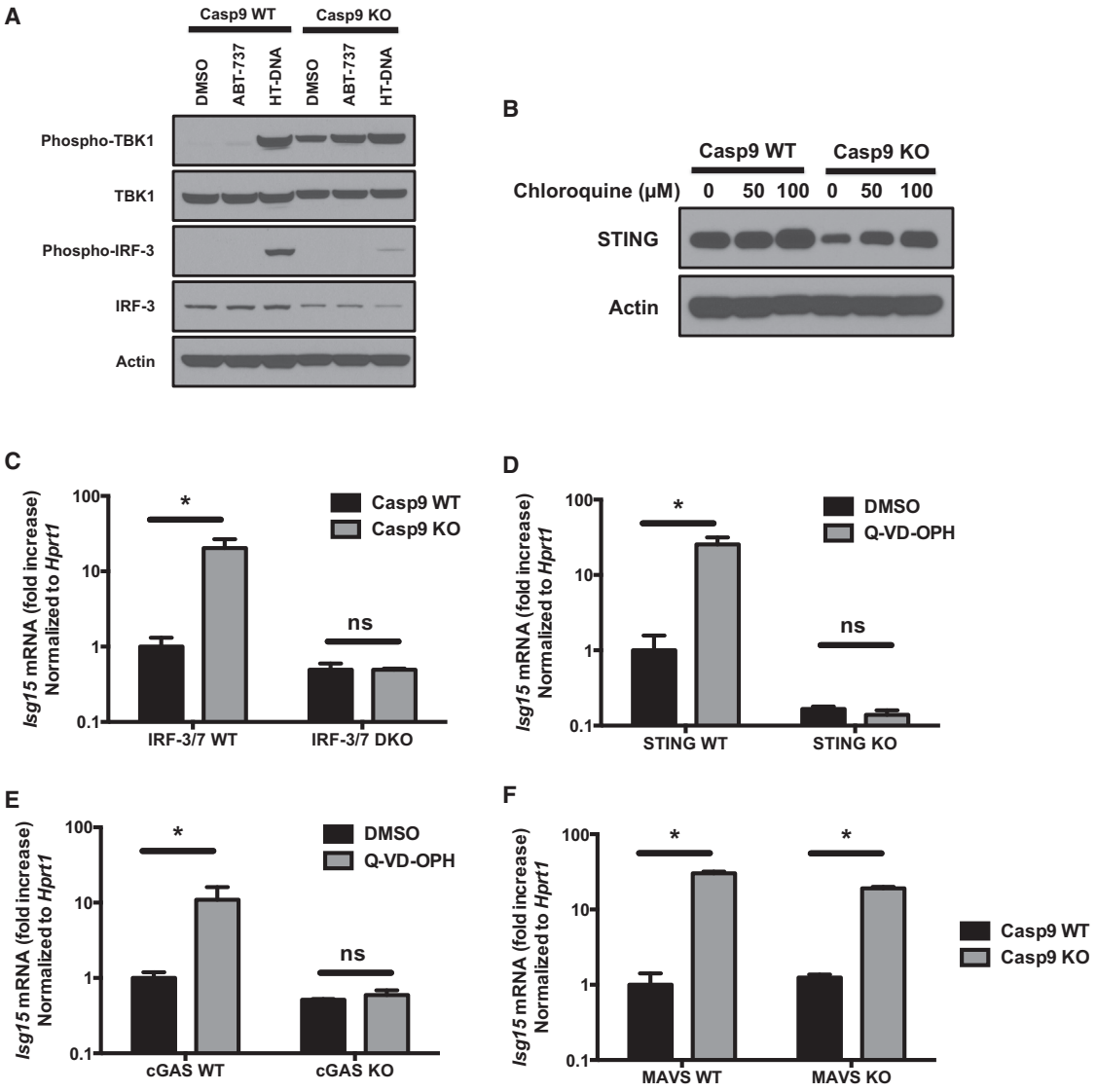

Figure 6. cGAS/STING-Dependent Constitutive ISG Expression in the Absence of Active Caspases

(A) Western blot analysis of the phosphorylation of TBK1 and IRF-3 in Casp9 WT and KO cells treated for 6 hr with vehicle (DMSO), with the Bcl-2 inhibitor ABT-737 (10 μM), or transfected with HT-DNA as a positive control (3 μg/ml, 3 hr). Result is representative of three independent experiments.

(B) Western blot analysis of STING in Casp9 WT and KO cells treated for 16 hr with the indicated concentrations of chloroquine.

(C) Caspase-9 KO mice were crossed with IRF-3/7 DKO, and the expression of ISG15 in embryo heads was measured by RT-PCR. Results shown are mean ± SD of three embryos for each genotype.

(D and E) STING WT and KO primary MEFs (D) or cGAS WT and KO bone-marrow-derived macrophages (E) were treated with vehicle (DMSO) or with the caspase inhibitor Q-VD-OPH (10 μM) and ISG expression was measured 48 hr later by RT-PCR (mean ± SD of triplicates, representative of two independent experiments).

(F) Caspase-9 KO mice were crossed with MAVS KO, and the expression of ISGs in embryo heads was measured by RT-PCR. Results shown are mean ± SD of two embryos for each genotype.

*$p < 0.05$; ns, not significant; pairwise comparisons following two-way ANOVA (C–F).

2008; Callus and Vaux, 2007; Tait et al., 2014). Those virally encoded caspase inhibitors represent an evolutionary response of viruses to host antiviral defenses (i.e., the suicide of infected cells) (Best, 2008; Callus and Vaux, 2007). Our model suggests that sensing caspase inhibition could be a mechanism by which host cells trigger an antiviral response independently of the physical sensing of viral nucleic acids.

Three important questions remain to be elucidated:

(1) What is the nature of the mtDNA involved, and how does it come into contact with cGAS? Given the size of the Bax/Bak pore, it is likely that small fragments of mtDNA, rather than entire copies of mitochondrial genome, are released. Because such fragments are experimentally difficult to

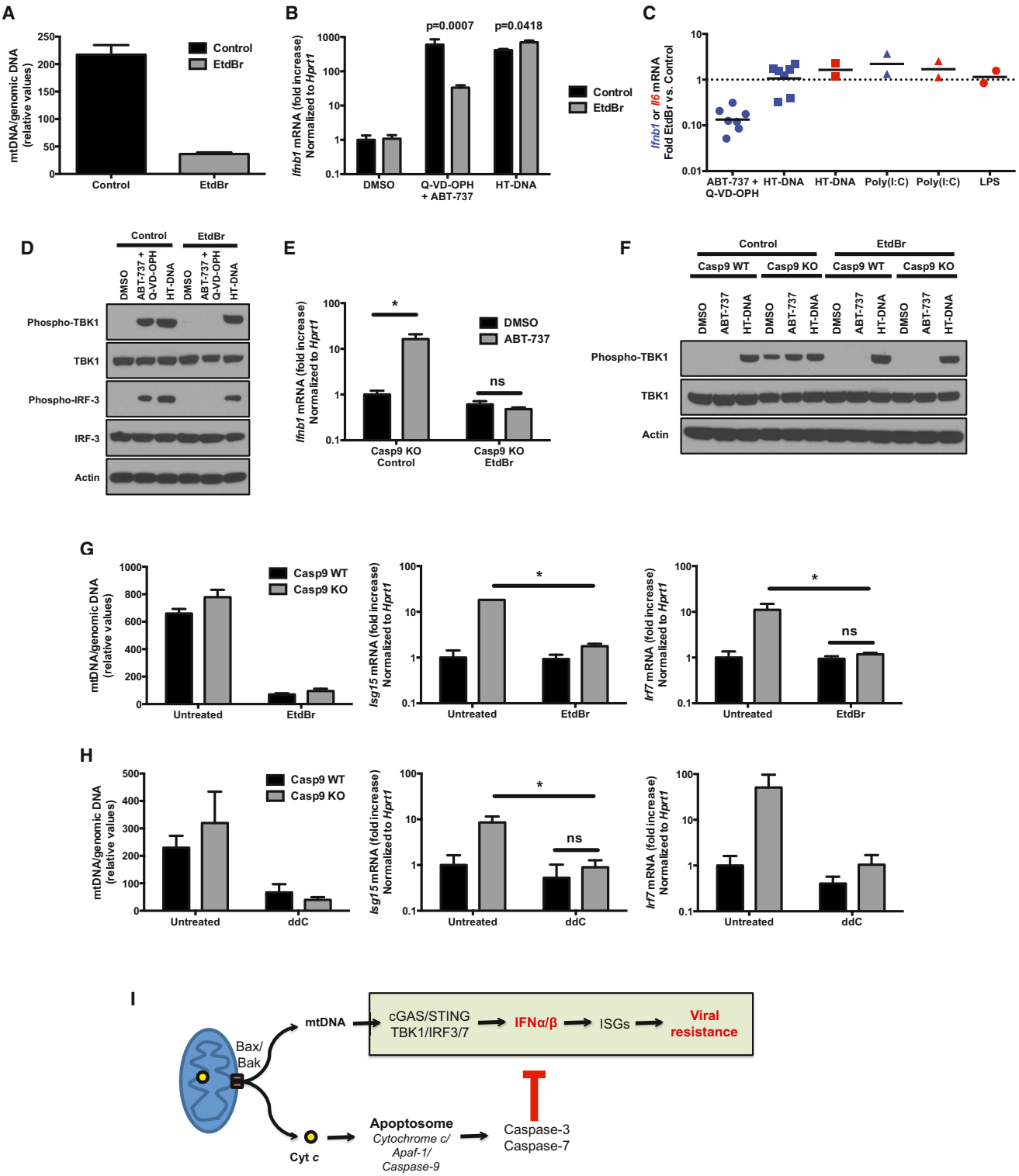

Figure 7. mtDNA Mediates the Induction of Type I IFN Expression

(A) Ratio of mitochondrial DNA (*dloop*) to genomic DNA (*Tert*) measured by RT-PCR on total extracts of WT immortalized MEFs treated for 4 days in EtdBr (150 ng/ml) and then maintained in culture for 16 hr without treatment (mean ± SD of duplicates, representative of at least five independent experiments).

(B) WT immortalized MEFs treated with EtdBr (150 ng/ml) as in (A) were stimulated with combined Bcl-2/caspase inhibitors (ABT-737 + Q-VD-OPH, 10 μM each) or transfected HT-DNA (3 μg/ml) for 6 hr, and the expression of IFNβ mRNA was measured by real-time RT-PCR (mean ± SD of duplicates). p values calculated by two-tailed unpaired Student's t test.

(legend continued on next page)

detect and to quantify reliably, further studies are needed to investigate this possibility. Studying the process of mtDNA release is complicated by the technical challenges of isolating cytosolic and mitochondrial fractions while maintaining the absolute integrity of mitochondria (without release of mtDNA) and of nucleic acids. Furthermore, our knowledge of the physiological mechanisms of mtDNA turnover and degradation is still incomplete (Clay Montier et al., 2009).

(2) How do caspases prevent mtDNA-dependent activation of the cGAS pathway? Our results suggest that caspases act upstream of STING activation. cGAS or a regulator of cGAS could be targets for caspase-dependent cleavage. Another possibility is that caspase-dependent nucleases (Nagata, 2005) could degrade mtDNA, thus preventing its binding to cGAS. Finally, caspases could affect the release of mtDNA from mitochondria.

(3) In which cells does this process occur in vivo? Dying cells, or cells that undergo incomplete MOMP and do not die, are the most probable source of Bax/Bak-dependent caspase-regulated type I IFNs. Alternatively, all cells could produce type I IFN at low levels and/or transiently due to leakiness of the Bax/Bak pore in healthy cells.

Answering those questions experimentally will require the development of novel experimental protocols that would allow the simultaneous monitoring of mtDNA release, of cGAS activity, and of caspase activation at the single-cell level.

A surprising observation is that caspase-deficient animals do not develop any symptoms of autoimmune disease, despite the constitutive activation of the type I IFN response. This observation suggests that caspase deficiency could affect the function of other aspects of the immune response. Future studies will determine how caspases contribute to the regulation of adaptive immunity and autoimmunity.

Finally, numerous pharmacological inhibitors of caspases have been developed and are being tested in clinical trials with the aim of preventing tissue damage caused by pathological cell death (Callus and Vaux, 2007). Our results suggest that the consequences of a chronic IFN response induced by these inhibitors should be evaluated. Conversely, we propose that caspase inhibitors could be used to induce an IFN response (i.e., the expression of ISGs) while minimizing the adverse effects caused by interferon therapies (Vilcek, 2006), as caspase inhibition induces only very low levels of type I IFNs.

It has long been known that apoptosis is an immunologically silent form of cell death, but the molecular basis of this is unknown. We demonstrate a role for mitochondria in the induction of a type I IFN-mediated cell intrinsic immune response in dying cells. Caspases, activated by mitochondria, are required to silence that immune process in apoptotic cells.

EXPERIMENTAL PROCEDURES

Mice

Conditional KO mice with a floxed caspase-9 allele or a floxed caspase-3 allele were generated as described in the Extended Experimental Procedures and illustrated in Figure S1. Caspase-9, caspase-3, caspase-7, Apaf-1, IFNAR1, IRF-3, IRF-7, MAVS, and cGAS (*Mb21d1*$^{-/-}$) -deficient mice have been reported previously (Honda et al., 2005; Kuida et al., 1996, 1998; Lakhani et al., 2006; Li et al., 2013; Müller et al., 1994; Sato et al., 2000; Sun et al., 2006; Yoshida et al., 1998). All animal experimentations were performed in compliance with Yale Institutional Animal Care and Use Committee protocols.

Cell Cultures

Primary MEFs were generated from caspase-9 KO, IFNAR1 KO, caspase-9/IFNAR1 double KO, caspases-3/-7 double KO, Apaf-1 KO, caspase-9/IRF-3/IRF-7 triple KO, and caspase-9/MAVS double KO and respective littermate control embryos (E16.5–E18.5). All primary MEFs used for experiments were from passage 4 or less. Bax/Bak double-KO and control immortalized MEFs were provided by Dr. C. Thompson (University of Pennsylvania) (Wei et al., 2001), and primary STING KO (*Tmem173*$^{-/-}$) MEFs were provided by Dr. G. Barber (University of Miami) (Ishikawa et al., 2009). SV40-immortalized Casp9 WT and KO MEFs were reported previously (Masud et al., 2007).

Herring testis DNA (HT-DNA, Sigma-Aldrich, 3 μg/ml) and poly(I:C) (Invivogen, 1 μg/ml) were transfected using Lipofectamine 2000 (Invitrogen, 3 μl/ml). IFNα (used at 50 U/ml) and anti-IFNα/β antibodies (used at 300 neutralizing U/ml each) were obtained from Hycult biotech and PBL Assay Science, respectively. Z-VAD-fmk, Boc-D-fmk (EMD Millipore), Q-VD-OPH (MP Biomedicals), and ABT-737 (SantaCruz Biotechnology) were used at 10 μg/ml. Staurosporine and Etoposide were obtained from Sigma-Aldrich and used at 0.01 μM or 10 μM, respectively.

Viral Infections

Mice were infected with EMCV by intraperitoneal injection of 2×10^3 $TCID_{50}$ of the virus diluted in 100 μl PBS. Mice were sacrificed and hearts were harvested 48 hr later, or survival was monitored for 27 days.

For VSV infection, mice were anesthetized with methoxyflurane (Anafane), and 10^6 PFU of VSV in 50 μl PBS were administered intranasally. The mice were sacrificed 24 hr later. Blood was collected by cardiac puncture and transferred in heparinized tubes. The samples were then centrifuged (2 min at 3,000 rpm), and dilutions of the plasma were used for viral titration.

(C) Fold inhibition by EtdBr pretreament of the induction of IFNβ (blue symbols) or IL-6 (red symbols) mRNA in cells stimulated with ABT-737 + Q-VD-OPH, transfected with HT-DNA, transfected with poly(I:C), or stimulated with LPS. Each dot represents an individual experiment.

(D) Western blot analysis of the phosphorylation of TBK1 and IRF-3 induced by ABT-737 + Q-VD-OPH (10 μM each, 6 hr) or by transfection of HT-DNA (3 μg/ml, 3 hr) in control WT immortalized MEFs or in the same cells pretreated as in (A) with EtdBr (450 ng/ml). Result representative of three independent experiments.

(E) Casp9 KO immortalized MEFs treated or not with EtdBr (450 ng/ml) as in (A) were stimulated with vehicle (DMSO) or the Bcl-2 inhibitor ABT-737 (10 μM) for 6 hr and the expression of IFNβ mRNA was measured by real-time RT-PCR (mean ± SD of duplicates, representative of two independent experiments).

(F) Western blot analysis of the phosphorylation of TBK1 after treatment with vehicle (DMSO) or the Bcl-2 inhibitor ABT-737 (10 μM, 6 hr) or after transfection of HT-DNA (3 μg/ml, 3 hr) in Casp9 WT and KO immortalized MEFs, pretreated or not with EtdBr (450 ng/ml) as in (A). Results are representative of three independent experiments.

(G and H) Casp9 WT and KO primary MEFs were treated for 4 days with EtdBr (150 ng/ml) (G), or immortalized MEFs were treated for 6 days with dideoxycytidine (ddC, 40 μg/ml) (H). The ratio of mitochondrial to genomic DNA was measured by real-time PCR on total extracts (left) and the expression of ISGs was determined by real-time RT-PCR. Results are shown as mean ± SD of triplicates, representative of three and two independent experiments, respectively.

(I) Schematic model representation of Bax/Bak-dependent, caspase-regulated activation by mtDNA of the cGAS/STING pathway of type I IFN induction.

*$p < 0.05$; ns, not significant; pairwise comparisons following two-way ANOVA (E, G, and H).

For in vitro infections, cells were plated at a density of 10^5 cells/ml in 6-well plates. The next day, the cells were infected with VSV-GFP, VSV-DsRed, HSV-2, or EMCV (diluted in 500 μl of DMEM without FBS) for 1 hr with gentle shaking every 15 min. The cells were then washed and incubated in 1 ml of media containing 10% FBS. The dose of virus used for infection and the duration of the incubation are indicated in figure legends.

Cell death was measured by flow cytometry after staining with Annexin V-APC and propidium iodide (BD Biosciences) or by LDH release assay (CytoTox 96 assay, Promega).

Type I IFN Bioassay

To measure type I IFN bioactivity, undiluted culture supernatants were transferred on cultures of the L929-pISRE-Luc reporter cell line (Jiang et al., 2005). The luciferase activity in cell lysates was measured 24 hr later (Dual-Luciferase Reporter Assay, Promega).

Mitochondrial DNA Depletion

Cells were treated with ethidium bromide (150 ng/ml or 450 ng/ml for 4 days; Sigma-Aldrich) or dideoxycytidine (40 μg/ml for 6 days; Sigma-Aldrich), RNA was extracted, and the expression of ISGs was measured by real-time RT-PCR. For induction of IFNβ expression by mtDNA-depleted cells, the cells were cultivated for 4 days in the presence of EtdBr, replated, cultivated overnight in the absence of EtdBr, and then stimulated as indicated. To measure the efficiency of mtDNA depletion, total extracts were prepared by resuspending the cells in NaOH 50 mM, incubation at 95°C for 1 hr, and neutralization by adding 10% volume Tris 1M (pH 7.5). The ratio of mtDNA (*dloop*) versus genomic DNA (*Tert*) was measured by SybrGreen real-time PCR using the following primer pairs:

dloop Forward: AATCTACCATCCTCCGTGAAACC
dloop Reverse: TCAGTTTAGCTACCCCCAAGTTTAA
Tert Forward: CTAGCTCATGTGTCAAGACCCTCTT
Tert Reverse: GCCAGCACGTTTCTCTCGTT

Statistical Analysis

The means of two groups were compared using two-tailed unpaired Student's t test. When three groups were compared, we used a one-way ANOVA test. When there were two variables, we used a two-way ANOVA test, followed by Games-Howell or Tukey post hoc test to compare pairs of means. Survival curves were compared using Mantel-Cox test.

ACCESSION NUMBERS

The GEO accession number for the RNA sequencing data reported in this paper is GSE63794.

SUPPLEMENTAL INFORMATION

Supplemental Information includes Extended Experimental Procedures, seven figures, and two tables and can be found with this article online at http://dx.doi.org/10.1016/j.cell.2014.11.037.

AUTHOR CONTRIBUTIONS

A.R., R.J., T.L., M.R.d.Z., and B.Y. performed experiments. A.R., R.J., C.C.D.H., and R.A.F. analyzed results. C.-Y.K., S.A.L., and A.R. generated conditional KO mice. A.P.W., Y.W., T.T., G.S.S., Z.J.C., and A.I. provided scientific advice and reagents. A.R. and R.A.F. conceived the project and wrote the manuscript. R.A.F. supervised the research.

ACKNOWLEDGMENTS

We thank C. Thompson, G. Barber, T. Mak, R. Medzhitov, B. Beutler, and R. Verma for providing reagents; A. Ferrandino, L. Evangelisti, J. Stein, and C. Hughes for ES cell work; F. Sutterwala and N. Palm for comments on the manuscript; J. Alderman for managerial support; and C. Lieber for manuscript submission. This work was funded by NIAID AI082030, DOD W81XWH-11-1-0745, and Blavatnik Family Foundation M157176 (to R.A.F.); by NIH R01-AI093967 and Cancer Prevention and Research Institute of Texas RP120718-P3 (to Z.J.C.); NIH R01-AG047632 and the United Mitochondrial Disease Foundation (to G.S.S.); by a Grant-In-Aid for Scientific Research on Innovative Areas from the Ministry of Education, Culture, Sports, Science, and Technology of Japan (to T.T.); and by a postdoctoral fellowship PF-13-035-01-DMC from the American Cancer Society (to A.P.W.). C.C.D.H. is a Howard Hughes Medical Institute International Student Research fellow. Z.J.C., A.I., and R.A.F. are Investigators of the Howard Hughes Medical Institute.

Received: June 10, 2014
Revised: October 3, 2014
Accepted: November 10, 2014
Published: December 18, 2014

REFERENCES

Best, S.M. (2008). Viral subversion of apoptotic enzymes: escape from death row. Annu. Rev. Microbiol. *62*, 171–192.

Cai, X., Chiu, Y.H., and Chen, Z.J. (2014). The cGAS-cGAMP-STING pathway of cytosolic DNA sensing and signaling. Mol. Cell *54*, 289–296.

Callus, B.A., and Vaux, D.L. (2007). Caspase inhibitors: viral, cellular and chemical. Cell Death Differ. *14*, 73–78.

Chipuk, J.E., and Green, D.R. (2005). Do inducers of apoptosis trigger caspase-independent cell death? Nat. Rev. Mol. Cell Biol. *6*, 268–275.

Chipuk, J.E., Moldoveanu, T., Llambi, F., Parsons, M.J., and Green, D.R. (2010). The BCL-2 family reunion. Mol. Cell *37*, 299–310.

Clay Montier, L.L., Deng, J.J., and Bai, Y. (2009). Number matters: control of mammalian mitochondrial DNA copy number. J. Genet. Genomics *36*, 125–131.

Fuchs, Y., and Steller, H. (2011). Programmed cell death in animal development and disease. Cell *147*, 742–758.

Gough, D.J., Messina, N.L., Clarke, C.J., Johnstone, R.W., and Levy, D.E. (2012). Constitutive type I interferon modulates homeostatic balance through tonic signaling. Immunity *36*, 166–174.

Hakem, R., Hakem, A., Duncan, G.S., Henderson, J.T., Woo, M., Soengas, M.S., Elia, A., de la Pompa, J.L., Kagi, D., Khoo, W., et al. (1998). Differential requirement for caspase 9 in apoptotic pathways in vivo. Cell *94*, 339–352.

Hashiguchi, K., and Zhang-Akiyama, Q.M. (2009). Establishment of human cell lines lacking mitochondrial DNA. Methods Mol. Biol. *554*, 383–391.

Honda, K., Yanai, H., Negishi, H., Asagiri, M., Sato, M., Mizutani, T., Shimada, N., Ohba, Y., Takaoka, A., Yoshida, N., and Taniguchi, T. (2005). IRF-7 is the master regulator of type-I interferon-dependent immune responses. Nature *434*, 772–777.

Ishikawa, H., Ma, Z., and Barber, G.N. (2009). STING regulates intracellular DNA-mediated, type I interferon-dependent innate immunity. Nature *461*, 788–792.

Jiang, X., and Wang, X. (2004). Cytochrome C-mediated apoptosis. Annu. Rev. Biochem. *73*, 87–106.

Jiang, Z., Georgel, P., Du, X., Shamel, L., Sovath, S., Mudd, S., Huber, M., Kalis, C., Keck, S., Galanos, C., et al. (2005). CD14 is required for MyD88-independent LPS signaling. Nat. Immunol. *6*, 565–570.

Kaguni, L.S. (2004). DNA polymerase gamma, the mitochondrial replicase. Annu. Rev. Biochem. *73*, 293–320.

Kawai, T., and Akira, S. (2011). Toll-like receptors and their crosstalk with other innate receptors in infection and immunity. Immunity *34*, 637–650.

Koni, P.A., Joshi, S.K., Temann, U.A., Olson, D., Burkly, L., and Flavell, R.A. (2001). Conditional vascular cell adhesion molecule 1 deletion in mice: impaired lymphocyte migration to bone marrow. J. Exp. Med. *193*, 741–754.

Konno, H., Konno, K., and Barber, G.N. (2013). Cyclic dinucleotides trigger ULK1 (ATG1) phosphorylation of STING to prevent sustained innate immune signaling. Cell *155*, 688–698.

Kroemer, G., Galluzzi, L., Kepp, O., and Zitvogel, L. (2013). Immunogenic cell death in cancer therapy. Annu. Rev. Immunol. *31*, 51–72.

Kroemer, G., Galluzzi, L., Vandenabeele, P., Abrams, J., Alnemri, E.S., Baehrecke, E.H., Blagosklonny, M.V., El-Deiry, W.S., Golstein, P., Green, D.R., et al.; Nomenclature Committee on Cell Death 2009 (2009). Classification of cell death: recommendations of the Nomenclature Committee on Cell Death 2009. Cell Death Differ. *16*, 3–11.

Kuida, K., Haydar, T.F., Kuan, C.Y., Gu, Y., Taya, C., Karasuyama, H., Su, M.S., Rakic, P., and Flavell, R.A. (1998). Reduced apoptosis and cytochrome c-mediated caspase activation in mice lacking caspase 9. Cell *94*, 325–337.

Kuida, K., Zheng, T.S., Na, S., Kuan, C., Yang, D., Karasuyama, H., Rakic, P., and Flavell, R.A. (1996). Decreased apoptosis in the brain and premature lethality in CPP32-deficient mice. Nature *384*, 368–372.

Kumar, S. (2007). Caspase function in programmed cell death. Cell Death Differ. *14*, 32–43.

Lakhani, S.A., Masud, A., Kuida, K., Porter, G.A., Jr., Booth, C.J., Mehal, W.Z., Inayat, I., and Flavell, R.A. (2006). Caspases 3 and 7: key mediators of mitochondrial events of apoptosis. Science *311*, 847–851.

Li, X.D., Wu, J., Gao, D., Wang, H., Sun, L., and Chen, Z.J. (2013). Pivotal roles of cGAS-cGAMP signaling in antiviral defense and immune adjuvant effects. Science *341*, 1390–1394.

Loo, Y.M., and Gale, M., Jr. (2011). Immune signaling by RIG-I-like receptors. Immunity *34*, 680–692.

Martin, S.J., Henry, C.M., and Cullen, S.P. (2012). A perspective on mammalian caspases as positive and negative regulators of inflammation. Mol. Cell *46*, 387–397.

Masud, A., Mohapatra, A., Lakhani, S.A., Ferrandino, A., Hakem, R., and Flavell, R.A. (2007). Endoplasmic reticulum stress-induced death of mouse embryonic fibroblasts requires the intrinsic pathway of apoptosis. J. Biol. Chem. *282*, 14132–14139.

Müller, U., Steinhoff, U., Reis, L.F., Hemmi, S., Pavlovic, J., Zinkernagel, R.M., and Aguet, M. (1994). Functional role of type I and type II interferons in antiviral defense. Science *264*, 1918–1921.

Nagata, S. (2005). DNA degradation in development and programmed cell death. Annu. Rev. Immunol. *23*, 853–875.

Oltersdorf, T., Elmore, S.W., Shoemaker, A.R., Armstrong, R.C., Augeri, D.J., Belli, B.A., Bruncko, M., Deckwerth, T.L., Dinges, J., Hajduk, P.J., et al. (2005). An inhibitor of Bcl-2 family proteins induces regression of solid tumours. Nature *435*, 677–681.

Riedl, S.J., and Salvesen, G.S. (2007). The apoptosome: signalling platform of cell death. Nat. Rev. Mol. Cell Biol. *8*, 405–413.

Saitoh, T., Tun-Kyi, A., Ryo, A., Yamamoto, M., Finn, G., Fujita, T., Akira, S., Yamamoto, N., Lu, K.P., and Yamaoka, S. (2006). Negative regulation of interferon-regulatory factor 3-dependent innate antiviral response by the prolyl isomerase Pin1. Nat. Immunol. *7*, 598–605.

Sato, M., Suemori, H., Hata, N., Asagiri, M., Ogasawara, K., Nakao, K., Nakaya, T., Katsuki, M., Noguchi, S., Tanaka, N., and Taniguchi, T. (2000). Distinct and essential roles of transcription factors IRF-3 and IRF-7 in response to viruses for IFN-alpha/beta gene induction. Immunity *13*, 539–548.

Schneider, W.M., Chevillotte, M.D., and Rice, C.M. (2014). Interferon-stimulated genes: a complex web of host defenses. Annu. Rev. Immunol. *32*, 513–545.

Stetson, D.B. (2009). Connections between antiviral defense and autoimmunity. Curr. Opin. Immunol. *21*, 244–250.

Stetson, D.B., and Medzhitov, R. (2006). Type I interferons in host defense. Immunity *25*, 373–381.

Sun, Q., Sun, L., Liu, H.H., Chen, X., Seth, R.B., Forman, J., and Chen, Z.J. (2006). The specific and essential role of MAVS in antiviral innate immune responses. Immunity *24*, 633–642.

Tait, S.W., and Green, D.R. (2010). Mitochondria and cell death: outer membrane permeabilization and beyond. Nat. Rev. Mol. Cell Biol. *11*, 621–632.

Tait, S.W., Ichim, G., and Green, D.R. (2014). Die another way—non-apoptotic mechanisms of cell death. J. Cell Sci. *127*, 2135–2144.

Tamura, T., Yanai, H., Savitsky, D., and Taniguchi, T. (2008). The IRF family transcription factors in immunity and oncogenesis. Annu. Rev. Immunol. *26*, 535–584.

Taniguchi, T., and Takaoka, A. (2001). A weak signal for strong responses: interferon-alpha/beta revisited. Nat. Rev. Mol. Cell Biol. *2*, 378–386.

Taylor, R.C., Cullen, S.P., and Martin, S.J. (2008). Apoptosis: controlled demolition at the cellular level. Nat. Rev. Mol. Cell Biol. *9*, 231–241.

Upton, J.W., and Chan, F.K. (2014). Staying alive: cell death in antiviral immunity. Mol. Cell *54*, 273–280.

Vanden Berghe, T., Linkermann, A., Jouan-Lanhouet, S., Walczak, H., and Vandenabeele, P. (2014). Regulated necrosis: the expanding network of non-apoptotic cell death pathways. Nat. Rev. Mol. Cell Biol. *15*, 135–147.

Vilcek, J. (2006). Fifty years of interferon research: aiming at a moving target. Immunity *25*, 343–348.

Wei, M.C., Zong, W.X., Cheng, E.H., Lindsten, T., Panoutsakopoulou, V., Ross, A.J., Roth, K.A., MacGregor, G.R., Thompson, C.B., and Korsmeyer, S.J. (2001). Proapoptotic BAX and BAK: a requisite gateway to mitochondrial dysfunction and death. Science *292*, 727–730.

Yatim, N., and Albert, M.L. (2011). Dying to replicate: the orchestration of the viral life cycle, cell death pathways, and immunity. Immunity *35*, 478–490.

Yoshida, H., Kong, Y.Y., Yoshida, R., Elia, A.J., Hakem, A., Hakem, R., Penninger, J.M., and Mak, T.W. (1998). Apaf1 is required for mitochondrial pathways of apoptosis and brain development. Cell *94*, 739–750.

Youle, R.J., and Strasser, A. (2008). The BCL-2 protein family: opposing activities that mediate cell death. Nat. Rev. Mol. Cell Biol. *9*, 47–59.